

Acetohydroxamate-Coordinated Oxovanadium(V) Complexes with Halide Containing Hydrazones: Synthesis, Characterization, X-ray Crystal Structures, and Antibacterial Activity

D. L. Peng^{a, b, *}

^aKey Laboratory of Surface and Interface Science of Henan Province, School of Material and Chemical Engineering, Zhengzhou University of Light Industry, Zhengzhou, 450001 P.R. China

^bHenan Collaborative Innovation Center of Environmental Pollution Control and Ecological Restoration, Zhengzhou University of Light Industry, Zhengzhou, 450001 P.R. China

*e-mail: pengdonglai2015@sina.com

Received April 25, 2019; revised July 10, 2019; accepted July 15, 2019

Abstract—Two oxovanadium(V) complexes, $[\text{VO}(\text{L})(\text{L}^1)]$ (**I**) and $[\text{VO}(\text{L})(\text{L}^2)]$ (**II**), where L = acetohydroxamate, H_2L^1 = 2-bromo- N' -(2-hydroxybenzylidene)benzohydrazide, H_2L^2 = 2-chloro- N' -(2-hydroxybenzylidene)benzohydrazide, have been synthesized by reaction of $\text{VO}(\text{Acac})_2$ with acetohydroxamic acid and hydrazone ligands, and characterized by elemental analyses, IR, UV-Vis, ^1H NMR, molar conductivity, and X-ray single crystal structural determination (CIF file CCDC nos. 1911887 (**I**), 1911888 (**II**)). The hydrazone ligands coordinate to the V atoms through phenolate oxygen, imino nitrogen, and enolate oxygen atoms. The acetohydroxamate ligand coordinate to the V atoms through the two oxygen atoms. The V atoms are in octahedral coordination with the sixth site coordinated by an oxo group. The antibacterial property of the complexes and the hydrazones against the bacteria *B. subtilis*, *E. coli*, *P. putida*, and *S. aureus* were studied. Both complexes exhibit remarkable antibacterial properties on *B. subtilis* and *S. aureus* comparable to Penicillin.

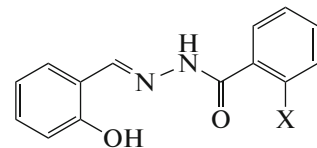
Keywords: hydrazone, oxovanadium(V) complex, X-ray diffraction, crystal structure, antibacterial activity

DOI: 10.1134/S1070328420040065

INTRODUCTION

Vanadium complexes with various ligands have received tremendous attention for their pharmacological activities [1–6], their potential to model vanadium-containing nitrogenases [7], and haloperoxidases [8, 9]. Amongst various classes of ligands, the biologically active Schiff bases have versatile coordination modes affording a large number of complexes with metal atoms [10–13]. Hydrazones, containing the typical functional group $-\text{CH}=\text{N}-\text{NH}-\text{C}(\text{O})-$ are a kind of Schiff bases. Hydrazones possess a broad spectrum of biological properties [14–18]. Metal complexes with hydrazones show interesting antibacterial properties [19–22]. Recent reports indicated that halide-containing groups of Schiff bases can increase the biological effects [23–25]. A literature survey reveals that vanadium complexes especially those with halide-containing hydrazones are scattered reported. In the present work, we have chosen two halide-containing hydrazones 2-bromo- N' -(2-hydroxybenzylidene)benzohydrazide (H_2L^1) and 2-chloro- N' -(2-hydroxybenzylidene)benzohydrazide (H_2L^2) as the precursor to prepare vanadium complexes with acetohydroxamic acid (HL) and $\text{VO}(\text{Acac})_2$. The free hydrazones and the newly prepared vanadium complexes

$[\text{VO}(\text{L})(\text{L}^1)]$ (**I**) and $[\text{VO}(\text{L})(\text{L}^2)]$ (**II**) have been screened for their antibacterial activity with a view to explore new and efficient biocidal agents.



$\text{H}_2\text{L}^1: \text{X} = \text{Br}; \text{H}_2\text{L}^2: \text{X} = \text{Cl}$

EXPERIMENTAL

Materials and methods. AR grade methanol was used as received. Salicylaldehyde, 2-chlorobenzohydrazide, 2-bromobenzohydrazide, and $[\text{VO}(\text{Acac})_2]$ were purchased from TCI. Microanalyses (C, H, N) were performed using a Perkin-Elmer 2400 elemental analyzer. Infrared spectra were measured on KBr disks with a Hitachi I-5040 FT-IR spectrophotometer. Electronic spectra were measured with a Lambda 35 spectrophotometer. Single crystal X-ray data were collected on a Bruker SMART APEX II CCD diffractometer. ^1H NMR was recorded on a Bruker 500 MHz instrument. The molar conductance (10^{-3} mol L^{-1})

Table 1. Crystallographic data and structure refinement for complexes **I** and **II**

Parameters	Value	
	I	II
Formula weight	458.14	413.68
Crystal system	Triclinic	Orthorhombic
Space group	$P\bar{1}$	$P2_12_1$
a , Å	8.0950(10)	8.031(1)
b , Å	9.7230(10)	10.955(1)
c , Å	12.8100(10)	19.792(1)
α , deg	71.9610(10)	90
β , deg	84.5450(10)	90
γ , deg	72.3720(10)	90
V , Å ³	913.67(16)	1741.3(3)
Z	2	4
ρ_{calcd} , g cm ⁻³	1.665	1.578
Crystal size, mm	0.26 × 0.23 × 0.20	0.31 × 0.27 × 0.23
$\mu(\text{Mo}K_{\alpha})$, mm ⁻¹	2.761	0.756
Min/max transmission	0.5338/0.6082	0.7994/0.8453
$F(000)$	456	840
Number of reflections	5535	11257
Unique reflections (R_{int})	3602 (0.0406)	3603 (0.0605)
Observed reflections ($I > 2\sigma(I)$)	1950	2794
Parameters	239	236
Restraints	7	0
Goodness of fit on F^2	1.050	1.099
R_1/wR_2 ($I > 2\sigma(I)$)	0.0823/0.2197	0.0486/0.1074
R_1/wR_2 (all data)	0.1431/0.2641	0.0752/0.1339

solutions in methanol) was determined on a DDS-11A conductivity meter at 25°C. The powder X-ray diffraction patterns (PXRD) of the complexes were recorded on a Bruker AXS D8 Advance diffractometer.

Synthesis of complex I. A methanol solution (10 mL) of $\text{VO}(\text{Acac})_2$ (0.1 mmol, 26.5 mg) was added to the methanol solution (10 mL) of H_2L^1 (0.1 mmol, 31.8 mg) and HL (0.1 mmol, 7.5 mg). The reaction mixture was stirred for 1 h at ambient temperature to give brown solution. Single crystals suitable for X-ray diffraction were obtained from the filtrate by slow

evaporation in a refrigerator. The yield was 27.8 mg (61%).

For $\text{C}_{16}\text{H}_{13}\text{N}_3\text{O}_5\text{BrV}$

Anal. calcd., % C, 41.95 H, 2.86 N, 9.17
Found, % C, 41.82 H, 2.95 N, 9.03

λ_{max} , nm (ϵ_{max} , L mol⁻¹ cm⁻¹) in methanol: 263 (18353), 322 (10670), 385 (2552). IR data (KBr, ν , cm⁻¹): 3205 (NH), 1610 (CH=N), 973 (V=O). ¹H NMR (500 MHz; DMSO-*d*⁶; δ , ppm): δ 13.92 (s,

1H, NH), 9.11 (s., 1H, CH=N), 7.78 (d., 1H, ArH), 7.72 (t., 2H, ArH), 7.57 (t., 1H, ArH), 7.49–7.41 (m., 2H, ArH), 7.02 (t., 1H, ArH), 6.90 (d., 1H, ArH), 2.13 (s., 3H, CH₃).

Synthesis of complex II. A methanol solution (10 mL) of VO(Acac)₂ (0.1 mmol, 26.5 mg) was added to the methanol solution (10 mL) of H₂L² (0.1 mmol, 27.4 mg) and HL (0.1 mmol, 7.5 mg). The reaction mixture was stirred for 1 h at ambient temperature to give brown solution. Single crystals suitable for X-ray diffraction were obtained from the filtrate by slow evaporation in a refrigerator. The yield was 23.2 mg (56%).

For C₁₆H₁₃N₃O₅ClIV

Anal. calcd., % C, 46.45 H, 3.17 N, 10.16
Found, % C, 46.28 H, 3.30 N, 9.98

λ_{max} , nm (ϵ_{max} , L mol⁻¹ cm⁻¹) in methanol: 260 (19125), 319 (12070), 390 (1960). IR data (KBr: λ , cm⁻¹): 3200 (NH), 1607 (CH=N), 965 (V=O). ¹H NMR (500 MHz; DMSO-*d*⁶; δ , ppm): 14.07 (s., 1H, NH), 9.25 (s., 1H, CH=N), 7.90 (d., 1H, ArH), 7.70 (t., 2H, ArH), 7.60 (t., 1H, ArH), 7.49–7.41 (m., 2H, ArH), 7.02 (t., 1H, ArH), 6.90 (d., 1H, ArH), 2.25 (s., 3H, CH₃).

X-ray crystallography. Data collection for the complexes was performed with a Bruker Apex II CCD diffractometer at 298 K. The structures were solved by direct methods with SHELXS-97 and refined by full-matrix least squares (SHELXL-97) on F^2 [26]. All non-hydrogen atoms were refined anisotropically. The amino hydrogen atoms were located from difference Fourier maps and refined with N–H restrained to 0.90(1) Å. The other hydrogen atoms were placed geometrically and refined with a riding model with isotropic displacement coefficients $U(\text{H}) = 1.2U(\text{C})$ or $1.5U(\text{C}_{\text{methyl}})$. Crystallographic data for the complexes are summarized in Table 1. Selected bond lengths and angles are listed in Table 2.

Supplementary material for structures has been deposited with the Cambridge Crystallographic Data Centre (CCDC nos. 1911887 (I) and 1911888 (II); deposit@ccdc.cam.ac.uk or www: <http://www.ccdc.cam.ac.uk>).

Antibacterial activity. The antibacterial activities were tested against *B. subtilis* ATCC 6633, *E. coli* ATCC 35218, *P. putida* TS 1138, and *S. aureus* ATCC 25923 using MH medium (Mueller–Hinton medium: casein hydrolysate 17.5 g, soluble starch 1.5 g, beef extract 1000 mL). The MICs (minimum inhibitory concentrations) of the test compounds were determined by a colorimetric method using the dye MTT [3-(4,5-dimethylthiazol-2-yl)-2,5-diphenyl tetrazolium bromide]. A stock solution of the synthesized compound (50 µg mL⁻¹) in DMSO was prepared and quantities of the test compounds were incorporated in

Table 2. Selected bond lengths (Å) and angles (deg) for complexes I and II

Bond	I	II
	<i>d</i> , Å	
V(1)–O(1)	1.968(5)	1.966(3)
V(1)–O(2)	1.822(6)	1.839(3)
V(1)–O(3)	1.879(5)	1.865(3)
V(1)–O(4)	2.217(5)	2.178(3)
V(1)–O(5)	1.601(5)	1.574(3)
V(1)–N(2)	2.108(6)	2.070(4)
Angle	ω , deg	
O(1)V(1)O(2)	156.1(2)	155.15(13)
O(1)V(1)O(3)	90.2(2)	92.29(13)
O(1)V(1)N(2)	74.4(2)	74.42(13)
O(2)V(1)N(2)	84.8(2)	84.17(13)
O(2)V(1)O(3)	105.5(2)	104.35(14)
O(4)V(1)O(1)	82.0(2)	81.79(13)
O(4)V(1)O(2)	84.4(3)	84.38(14)
O(4)V(1)O(3)	76.3(2)	76.23(13)
O(4)V(1)N(2)	84.4(2)	86.15(13)
O(5)V(1)O(1)	96.3(3)	97.33(17)
O(5)V(1)O(2)	100.2(3)	98.95(17)
O(5)V(1)O(3)	94.3(3)	96.44(17)
O(5)V(1)O(4)	170.4(3)	172.55(15)
O(5)V(1)N(2)	104.3(3)	100.77(17)
N(2)V(1)O(3)	156.9(2)	159.38(14)

specified quantity of sterilized liquid MH medium. A specified quantity of the medium containing the compound was poured into microtitration plates. A suspension of the microorganism was prepared to contain approximately 10⁵ cfu mL⁻¹ and applied to microtitration plates with serially diluted compounds in DMSO to be tested and incubated at 37°C for 24 h. After the MICs were visually determined on each of the microtitration plates, 50 µL of PBS (phosphate buffered saline 0.01 mol L⁻¹, pH 7.4: Na₂HPO₄ 2.9 g, KH₂PO₄ 0.2 g, NaCl 8.0 g, KCl 0.2 g, distilled water 1000 mL) containing 2 mg of MTT per mL⁻¹ was added to each well. Incubation was continued at room temperature for 4–5 h. The content of each well was removed and 100 µL of isopropanol containing 5% 1 mol L⁻¹ HCl was added to extract the dye. After 12 h of incubation at room temperature, the optical density was measured with a microplate reader at 550 nm.

RESULTS AND DISCUSSION

Reaction of VO(Acac)₂ with the hydrazones H₂L² and H₂L¹ in methanol, respectively, generated the

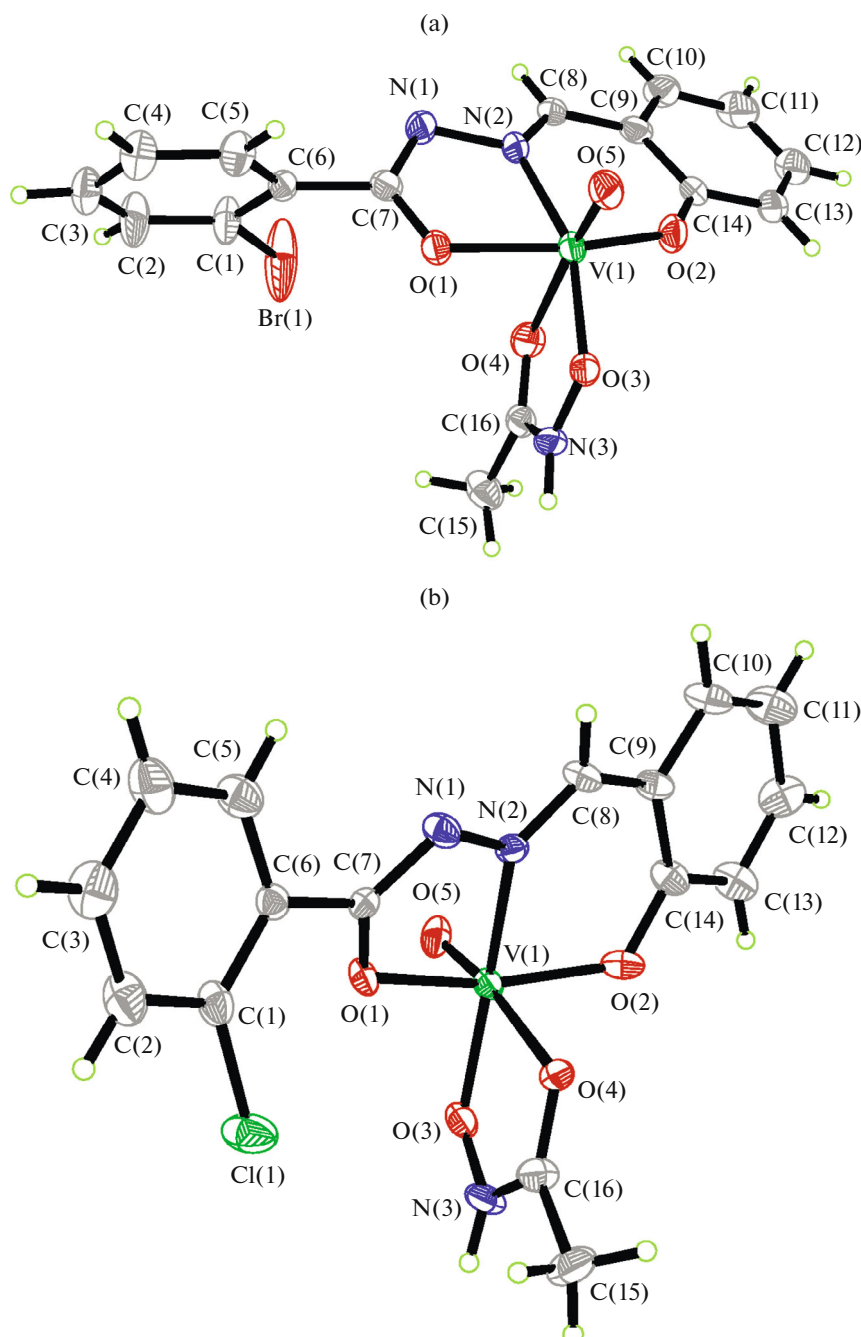


Fig. 1. Molecular structures of complexes I (a) and II (b).

complexes with formulae $[\text{VO}(\text{L})(\text{L}^1)]$ for I and $[\text{VO}(\text{L})(\text{L}^2)]$ for II. The complexes crystallized as deep brown, and soluble in methanol, ethanol, acetonitrile, DMSO, DMF, etc. Molar conductance values of the complexes in methanol are $12\text{--}19 \Omega^{-1} \text{cm}^2 \text{mol}^{-1}$ for the complexes, indicating non-electrolytes.

The molecular structures of the complexes are shown in Fig. 1. The V atoms are in octahedral geometry, coordinated by the three donor atoms (O(1), O(2), N(2)) of the hydrazone ligands, the oxygen

atoms (O(3), O(4)) of the acetoxyhydroxamate ligands, and the oxo groups (O(5)). The three donor atoms of the hydrazone ligands and the O(3) atom of the acetoxyhydroxamate ligands defining the equatorial planes of the octahedral geometries, and with the remaining two donor atoms located at the axial positions. The bond distances subtended at the V atoms in both complexes are comparable to each other, and within normal values when compared with reported vanadium complexes [27, 28]. The V=O distances are 1.57–1.60 Å. The V atoms are displaced by 0.286(2) Å (I) and

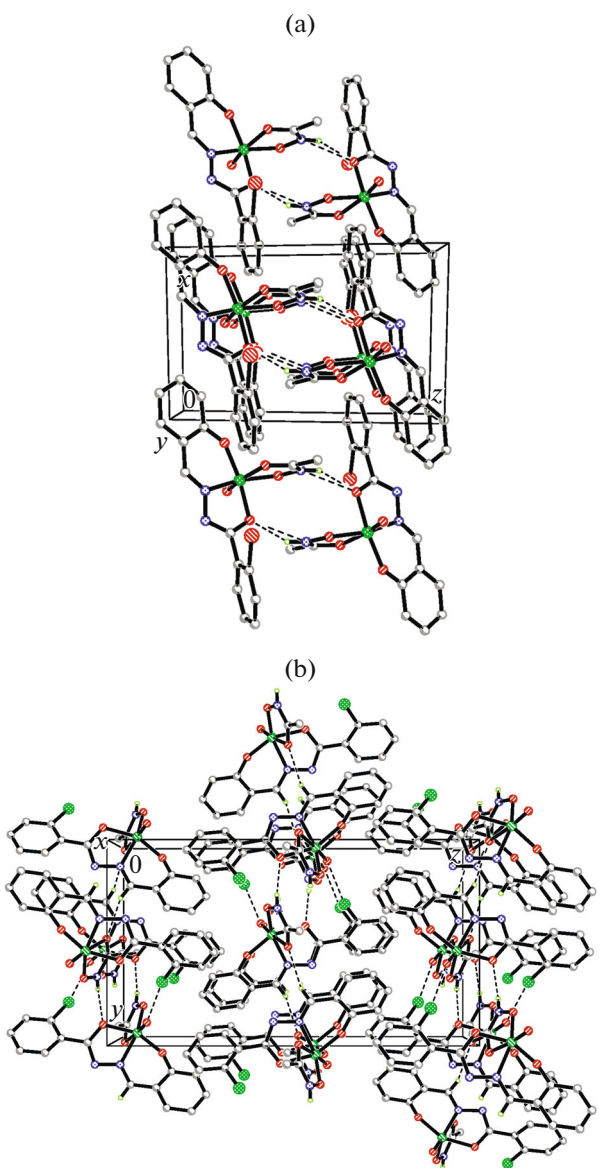


Fig. 2. Molecular packing structures of complexes **I** (a) and **II** (b). Hydrogen bonds are shown as dashed lines.

0.275(2) Å (**II**) from the mean plane defined by the donor atoms O(1), O(2), O(3), and N(2) towards the oxo groups. The tridentate O,N,O donor ligands form one five-membered and one six-membered chelate rings with bite angles of about 74° (O(2)V(1)N(1)) and 84° (N(1)V(1)O(1)). The *cis* and *trans* coordinate bond angles are range from 74.4° to 105.5° and from 156.1° to 170.4° for **I**, and from 74.4° to 104.4° and from 155.1° to 172.6° for **II**, respectively, indicating the distortion of the octahedral coordination from ideal geometry.

The crystal structures of the complexes are shown in Fig. 2. The molecules in complex **I** are linked through hydrogen bonds (Table 3) to form dimers. The molecules in complex **II** are linked through

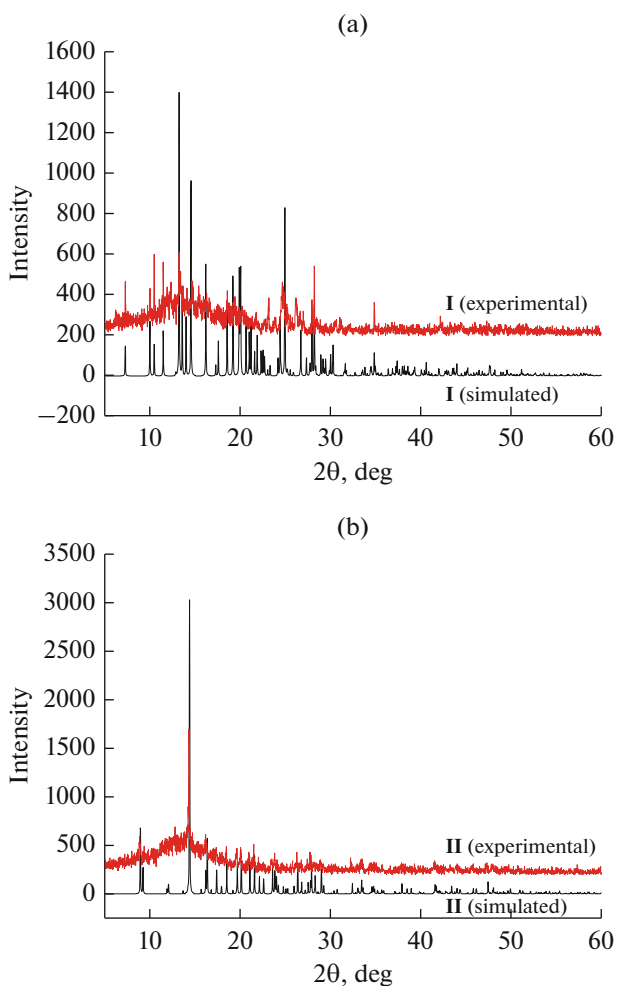


Fig. 3. Experimental and simulated powder XRD patterns of **I** and **II**.

hydrogen bonds (Table 3) to form layers along the xy plane.

The experimental PXRD patterns of the bulk samples of the complexes agree well with the simulated patterns calculated from singlecrystal X-ray diffraction (Fig. 3). The results prove the purity of the bulk samples.

The spectra of the complexes are shown in Fig. 4. The absence of the bands due to the N–H stretching in the spectra of the complexes indicates enolization and deprotonation of the amide functionality upon coordination to the V atoms. The strong bands corresponding to the azomethine groups ($\text{CH}=\text{N}$) are observed at about $1607\text{--}1610\text{ cm}^{-1}$ [29]. The typical absorptions for the $\text{V}=\text{O}$ groups are observed at $965\text{--}973\text{ cm}^{-1}$ [30]. The spectra of the complexes have weak bands at $3200\text{--}3205\text{ cm}^{-1}$, which can be assigned to the stretching vibration of the N–H groups of the acetoxyhydroxamate ligands.

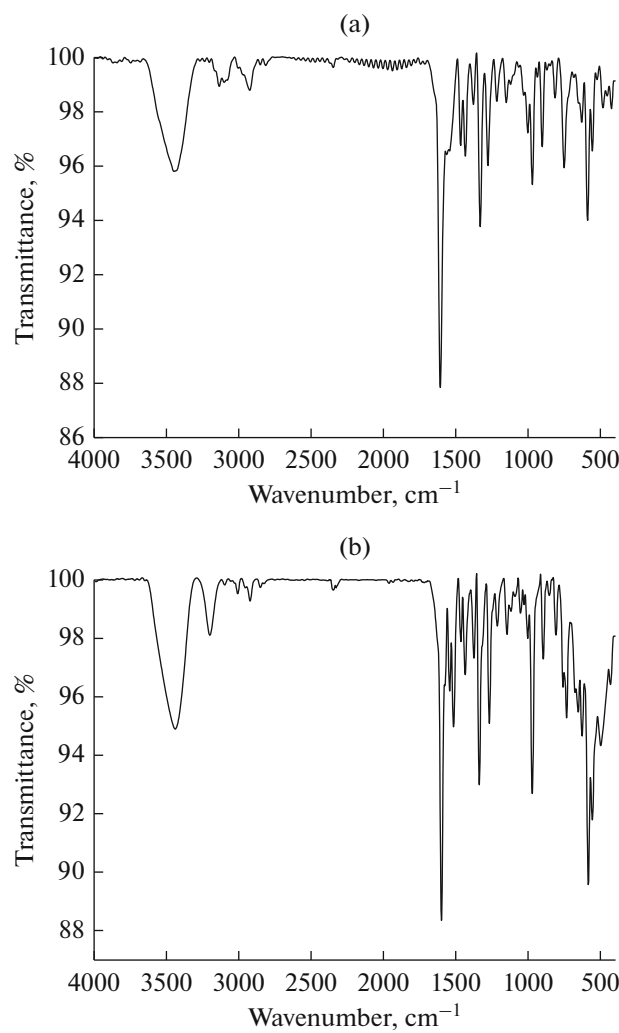


Fig. 4. IR spectra of complexes I (a) and II (b).

The electronic spectra of the complexes are shown in Fig. 5. The band at about 260 nm is most likely due to a transition involving ligand orbitals only [31]. The lowest energy transition at about 390 nm for the complexes are attributed to the intra-molecular charge transfer transitions from the p_{π} orbital on the phenoxy O to the empty d orbitals of the V atoms [28].

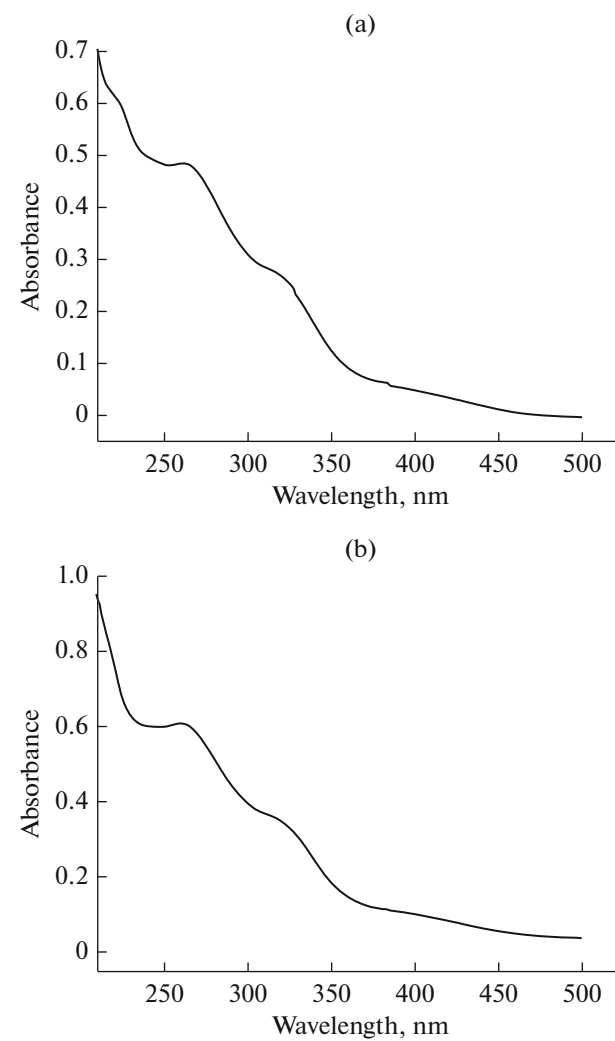


Fig. 5. Electronic spectra of complexes I (a) and II (b).

The complexes and the free hydrazones were screened for antibacterial activity against *B. subtilis* ATCC 6633, *E. coli* ATCC 35218, *P. putida* TS 1138, and *S. aureus* ATCC 25923 by the MTT method. The MIC values of the complexes against these bacteria are presented in Table 4. The antibiotic Penicillin was included as a reference. In general, both complexes have more effective activities against the bacteria than

Table 3. Geometric parameters of hydrogen bond for complexes I and II*

$D-H\cdots A$	Distances, Å			Angle ($D-H\cdots A$), deg
	$D-H$	$H\cdots A$	$D\cdots A$	
N(3)-H(3)…O(1) ^{#1}	0.90	1.97(5)	2.787(7)	150(8)
N(3)-H(3)…O(1) ^{#2}	0.86	2.14(3)	2.970(5)	162(6)
C(8)-H(8)…O(4) ^{#3}	0.93	2.44(3)	3.326(5)	160(6)

* Symmetry codes: ^{#1} 1 - x , 2 - y , 1 - z ; ^{#2} -1/2 + x , 3/2 - y , - z ; ^{#3} 1/2 + x , 1/2 - y , - z .

Table 4. MIC ($\mu\text{g mL}^{-1}$) values of the antibacterial activity of the compounds

Compound	<i>B. subtilis</i>	<i>E. coli</i>	<i>P. putida</i>	<i>S. aureus</i>
H ₂ L ¹	12.5	>100	>100	6.25
H ₂ L ²	6.25	>100	>100	6.25
I	0.78	50	25.0	3.12
II	0.39	50	25.0	1.56
Penicillin	0.78	>100	12.5	3.13

the free hydrazones. It is interesting that for *B. subtilis* and *S. aureus*, the complexes have strong activities with MIC values of 0.78 and 3.12 $\mu\text{g mL}^{-1}$ for **I** and 0.39 and 1.56 $\mu\text{g mL}^{-1}$ for **II**. As for *E. coli* and *P. putida*, the complexes also have antibacterial activities, but they are not efficiency. Thus, the complexes are active on *B. subtilis* and *S. aureus*, which deserve further study.

Thus, two oxovanadium(V) complexes derived from 2-bromo-*N'*-(2-hydroxybenzylidene)benzohydrazide and 2-chloro-*N'*-(2-hydroxybenzylidene)benzohydrazide have been synthesized and characterized. Single crystal X-ray determination indicates that the V atoms are in octahedral coordination. The complexes are active on the antibacterial property against *B. subtilis* and *S. aureus*.

ACKNOWLEDGMENTS

This work was supported by Zhengzhou University of Light Industry.

REFERENCES

1. Barfeie, H., Grivani, G., Eigner, V., et al., *Polyhedron*, 2018, vol. 146, p. 19.
2. Kolesa-Dobravc, T., Maejima, K., Yoshikawa, Y., et al., *New J. Chem.*, 2018, vol. 42, no. 5, p. 3619.
3. Jakusch, T., Kozma, K., Enyedy, E.A., et al., *Inorg. Chim. Acta*, 2018, vol. 472, p. 243.
4. Reytman, L., Hochman, J., and Tshuva, E.Y., *J. Coord. Chem.*, 2018, vol. 71, nos. 11–13, p. 2003.
5. Sultan, S., Ashiq, U., Jamal, R.A., et al., *Biometals*, 2017, vol. 30, no. 6, p. 873.
6. Heidari, F., Fatemi, S.J.A., Ebrahimipour, S.Y., et al., *Inorg. Chem. Commun.*, 2017, vol. 76, p. 1.
7. Kober, E., Janas, Z., and Jezierska, J., *Inorg. Chem.*, 2016, vol. 55, no. 21, p. 10888.
8. Mba, M., Pontini, M., Lovat, S., et al., *Inorg. Chem.*, 2008, vol. 47, no. 19, p. 8616.
9. Smith, T.S. and Pecoraro, V.L., *Inorg. Chem.*, 2002, vol. 41, no. 25, p. 6754.
10. Kaczmarek, M.T., Zabiszak, M., Nowak, M., et al., *Coord. Chem. Rev.*, 2018, vol. 370, p. 42.
11. Liu, X., Manzur, C., Novoa, N., et al., *Coord. Chem. Rev.*, 2018, vol. 357, p. 144.
12. Zhang, J., Xu, L.L., and Wong, W.-Y., *Coord. Chem. Rev.*, 2018, vol. 355, p. 180.
13. Rezaeivala, M. and Keypour, H., *Coord. Chem. Rev.*, 2014, vol. 280, p. 203.
14. El-Sherif, A.A., Fetoh, A., Abdulhamed, Y.K., et al., *Inorg. Chim. Acta*, 2018, vol. 480, p. 1.
15. Abdalgawad, M.A., Labib, M.B., and Abdel-Latif, M., *Bioorg. Chem.*, 2017, vol. 74, p. 212.
16. Shankar, R., Rawal, R.K., Singh, U.S., et al., *Med. Chem. Res.*, 2017, vol. 26, no. 7, p. 1459.
17. Karaman, N., Sicak, Y., Taskin-Tok, T., et al., *Eur. J. Med. Chem.*, 2016, vol. 124, p. 270.
18. Amato, J., Morigi, R., Pagano, B., et al., *J. Med. Chem.*, 2016, vol. 59, no. 12, p. 5706.
19. Fekri, R., Salehi, M., Asadi, A., et al., *Inorg. Chim. Acta*, 2019, vol. 484, p. 245.
20. Bera, P., Brando, P., Mondal, G., et al., *Polyhedron*, 2017, vol. 134, p. 230.
21. Sharma, N., Kumari, M., Kumar, V., et al., *J. Coord. Chem.*, 2010, vol. 63, no. 11, p. 1940.
22. Sedaghat, T., Yousefi, M., Bruno, G., et al., *Polyhedron*, 2014, vol. 79, p. 88.
23. Zhang, M., Xian, D.-M., Li, H.-H., et al., *Aust. J. Chem.*, 2012, vol. 65, no. 4, p. 343.
24. Gopalakrishnan, M., Thanusu, J., Kanagarajan, V., et al., *J. Enzym. Inhib. Med. Chem.*, 2009, vol. 24, no. 1, p. 52.
25. Shi, L., Ge, H.-M., Tan, S.-H., et al., *Eur. J. Med. Chem.*, 2007, vol. 42, no. 4, p. 558.
26. Sheldrick, G.M., *Acta Crystallogr., Sect. C: Struct. Chem.*, 2015, vol. 71, no. 1, p. 3.
27. Qian, H.Y., *Russ. J. Coord. Chem.*, 2017, vol. 43, no. 11, p. 780.
<https://doi.org/10.1134/S107032841711007>
28. Zhu, X.W., *Russ. J. Coord. Chem.*, 2018, vol. 44, no. 5, p. 335.
<https://doi.org/10.1134/S1070328418050081>
29. Yu, H., Guo, S., Cheng, J.-Y., et al., *J. Coord. Chem.*, 2018, vol. 71, no. 24, p. 4164.
30. Guo, S., Sun, N., Ding, Y., et al., *Z. Anorg. Allg. Chem.*, 2018, vol. 644, no. 19, p. 1172.
31. Sarkar, A. and Pal, S., *Polyhedron*, 2006, vol. 25, p. 1689.